Effect of Nonlinear Radiative Heat and Mass Transfer on MHD Flow Over A Stretching Surface with Variable Conductivity and Viscosity

[1]A.M. Okedoye, [2]S.O. Salawu and [2]A. Abolarinwa
[1]*Department of Mathematics and Computer Science, Federal University of Petroleum Resources, Effurun, Nigeria*
[2]*Department of Mathematics, Landmark University, Omu-Aran, Nigeria*

Abstract: A theoretical investigation on the flow of nonlinear MHD, laminar, viscous, incompressible boundary layer fluid with thermal radiative heat transfer and variable properties past a stretching plate was carried out. The liquid is taken to be gray, absorbing, emitting but with non-scattering medium. The main nonlinear equations governing the flow are reduced to ordinary differential equations by using appropriate similarity variables and quantities. The obtained nonlinear equations are computational solved by applying shooting techniques coupled with Nachtsheim-Swigert method for asymptotic satisfaction of boundary conditions by fourth order Runge-Kutta scheme. The computational results for momentum and heat distribution are gotten for various values of the emerging parameters. The results for the coefficient of skin friction and dimension less heat gradient are likewise obtained for different physical parameters values. From the study, it was observed that the parameters which enhance the heat source terms decreases the fluid viscosity and causes increase in the flow rate. Also, parameter that reduces heat source terms encourages viscosity which resulted in retardation of the fluid velocity.

Corresponding Author:
A.M. Okedoye
Department of Mathematics and Computer Science, Federal University of Petroleum Resources, Effurun, Nigeria

INTRODUCTION

It is an established contention that several industrial and engineering processes involving heat and mass transport such as glass fibre, metal extrusion, rubber manufacturing and many more takes place in the presence of simultaneously effects of thermal and species buoyancy forces. Different studies on the fluid flow through an inclined, horizontal and vertical surface in the existence of magnetic field have been examined. By Seth *et al*.[1]

and Salawu and Oke[2] the analysis of dissipative heat transfer of hydromagnetic fluid flow past an inclined plate was investigated. Salawu and Okedoye[3] investigated gravity driven flow of reactive hydromagnetic fluid through a vertical channel in the presence of magnetic field. Hassan *et al*.[4] studied hydro magnetic reactive fluid flow through horizontal porous plates with radiation and internal heat generation.

Fluids flow past a vertical Couette boundary layer plates with heat radiation is gaining considerable

attraction due to its wide spectrum usefulness in industrial systems. For example, it useful in the rocket engine, combustion chamber, geo thermal reservoirs, thermal insulation and so on. Various leading past studies concerning convection flow through vertical plates in the presence radiation has been established in the research work by Fetecau *et al*.[5], Hayat *et al*.[6], Salawu *et al*.[7] and Devi and Gururaj[8]. The heat transfer in over a stretching plate is important in several devices and industrial applications. In manufacturing process of rubber and plastic sheet where it is frequently important to blow gaseous through the unsolidi fied material, this circumstance emerge in the glass blowing, expulsion processes and spinning of fibers also include the flow as a result of stretching plate Hayat *et al*.[6], Salawu *et al*.[7] and Devi and Gururaj[8] reported on heat transport characteristics of two dimensional nonlinear hydromagnetic incompressible fluids with variable viscosity and electrically conductivity. The liquid is taken to be gray, absorbing, emitting but not scattering medium. By Gitima[9], the influence of radiation on the flow of boundary layer in the existence of magnetic field with thermal conductivity and variable viscosity due to an stretching surface in a permeable medium was investigated. To show the heat flux by radiation in the heat equation, Rosseland approximation was utilized. The energy and species transport through a vertical surface under the joined effect of the diffusion thermo and thermo diffusion in the existence of magnetic field was carried out by Hazarika and Ch[10]. A computational solution of a convective transient fluid flow with thermal radiation over a moving plate of a Sisko binary fluid was analyzed by Okedoye[11]. The problem formulated was solved numerically; the outcomes of the analysis demonstrated that the flow is affected considerably by the injection/suction, heat source and chemical reaction at the plate surface. Also, the impact of Soret and Dufour on a Sisko fluid is significant.

The understanding of the thermophysics properties of some parameters associated with the fluid flows with temperature dependent variable properties have instant influences on the micro fluidics, ink-jet printing, polymer production, earth mantle geological flows, colloidal flow suspensions, turbulent flow shear, fluid gems and many more. In respect of this, scientist has being showing high interest on the intrigue behavior of fluids with variable properties and subsequently studies has been done on it using the analytical and computational approaches which are available in many articles including[15-17]. A few great reports on the flow of fluid through a stretching surface are presented by Afify[18], Abdou *et al*.[19], Yurusoy[20], Grubka and Bobba[21] and Ali[22]. Considering the above studies, the researchers ignored the heat dependent

thermal conductivity and viscosity in the momentum variation power-law. The variable physical properties may vary meaningfully with changes in temperature, when taken into variable properties into consideration. The present study aims to investigate heat dependent variable properties with variable surface velocity over a stretching plate. The flow is propelled by the influence of buoyancy forces in the existence of thermal radiation in a stretching plate.

MATERIALS AND METHODS

Formulation of the problem: Forced convection flow of nonlinear radiation along a stretching horizontal plate kept at the same wall temperature. The stretching surface is with velocity power law of (where and are constants) through a fluid with variable viscosity is considered. The electrically conducting fluid is taken to be incompressible, viscous, absorbing, emitting, gray and non-scattering medium with temperature. A magnetic field is assumed perpendicular to flow in a horizontal stretching surface. Cartesian coordinate system is chosen. The main flow is along axis direction in a stretching sheet with velocity components and in these directions[18, 23, 24]. The flow runs continuously along the x-axis with y-axis normal to it. The assumptions below are considered (Fig. 1):

- The flow is laminar, steady in two-dimensional
- Excluding the viscosity of the fluid, the fluid thermophysical properties are taken be unchanged
- The induced magnetic and Reynolds number are considered negligible and small, respectively
- The Joule's heating and heat viscous is taken to be negligible
- The heat flux radiation is considered negligible in the x-direction compared to they-direction

The continuity, momentum and energy conservation equations under the above assumptions are presented as:

$$\frac{\partial u}{\partial x} + \frac{\partial u}{\partial y} = 0 \tag{1}$$

$$\rho\left(u\frac{\partial u}{\partial x} + v\frac{\partial u}{\partial y}\right) = \frac{\partial}{\partial y}\left(\mu\frac{\partial u}{\partial y}\right) + g\beta\tau\left(T\text{-}T_\infty\right) + \\ g\beta c\left(C\text{-}C_\infty\right)\text{-}\sigma B_0^2 u \tag{2}$$

$$\rho c_p\left(u\frac{\partial T}{\partial x} + v\frac{\partial T}{\partial y}\right) = \frac{\partial}{\partial y}\left(k_*\frac{\partial T}{\partial y}\right) + \frac{\partial q_r}{\partial y} \tag{3}$$
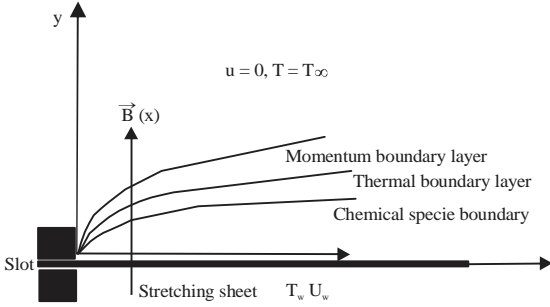
Fig. 1: Schematic diagram of the problem

$$\rho\left(u\frac{\partial C}{\partial x}+v\frac{\partial C}{\partial y}\right)=\frac{\partial^2 C}{\partial y^2}+A(C-C_\infty) \qquad (4)$$

The fluid viscosity is taken as:

$$\frac{1}{\mu}=d_2(T-T_r) \qquad (5)$$

where, $d_2 = d_1/\mu_\infty$, $T_r = T_\infty-1/d_1$ and $B(x) = B_0 x^{m-1/2}$. Here, d_1, d_2 and T_r are constants and their values depend on the fluid thermal property and the reference state. The associated boundary conditions are:

$$u = u_w = u_0 x^m, v = 0, T = T_w \text{ at } y = 0 (u_0 > 0)$$
$$u = 0, T = T_\infty \text{ as } y \to \infty \qquad (6)$$

Where:

u_w : The velocity of the stretching surface, the components velocity are respectively the quantities u and v the direction of x

y, u_0 : A constant

B_0 : The magnetic field and all the other quantities have their usual meanings

The heat flux radiativeterm is defined by using the Rosseland diffusion approximation, Salawu and Dada[25]:

$$q_r = -\frac{16\sigma^* T^3}{3\alpha^*}\frac{\partial T}{\partial y} \qquad (7)$$

Where:

σ^* : The Boltzmann-Stefan constant

α^* : The coefficient mean Rosseland absorption

Using the stream function, $\psi(x, y)$ the continuity equation is satisfied such that:

$$u = \frac{\partial \psi}{\partial y} \text{ and } v = -\frac{\partial \psi}{\partial x}$$

Applying the suitable similarity transformation[26]:

$$\eta(x, y) = y\sqrt{\frac{m+1}{2}}\sqrt{\frac{u_0 x^{m-1}}{\upsilon}}$$

$$\psi(x, y) = y\sqrt{\frac{2}{m+1}}\sqrt{\upsilon u_0 x^{m+1}}f(\eta)$$

$$\theta(\eta) = \frac{T-T_\infty}{T_w-T_\infty}, \theta_w = \frac{T_w}{T_\infty}$$

where, θ_w is surface temperature parameter. Now:

$$q_r = -\frac{16\sigma^* T^3}{3\alpha^*}\frac{\partial T}{\partial y} = -\frac{16\sigma^* T^3}{3\alpha^*}(T_w-T_\infty)\sqrt{\frac{m+1}{2}}\sqrt{\frac{u_0 x^{m-1}}{\upsilon}}$$

$$\left(\left(\frac{T_w}{T_\infty}-1\right)\theta+1\right)^3\left(\frac{T_w}{T_¥}-1\right)\frac{d\theta}{d\eta} = -\frac{16\sigma^* T^4}{3\alpha^*}$$

$$\sqrt{\frac{m+1}{2}}\sqrt{\frac{u_0 x^{m-1}}{\upsilon}}\left(\left(\frac{T_w}{T_0}-1\right)\theta+1\right)^3\left(\frac{T_w}{T_\infty}-1\right)^2\frac{d\theta}{d\eta}$$

Since:

$$\theta_w = \frac{T_w}{T_\infty}, \text{ let } \theta_w = \bar{\theta}_w+1$$

$$q_r = -\frac{16\sigma^* T^4}{3\alpha^*}\sqrt{\frac{m+1}{2}\frac{u_0 x^{m-1}}{\upsilon}}\left(\theta\bar{\theta}_w+1\right)^3\bar{\theta}_w^2\frac{d\theta}{d\eta}$$

Thus:

$$\frac{\partial q_r}{\partial y} = \frac{dq_r}{d\eta}\frac{d\eta}{dy} = -\frac{16\sigma^* T^4}{3\alpha^*}\frac{m+1}{2}\frac{u_0 x^{m-1}}{\upsilon}\bar{\theta}_w$$
$$\left(3\bar{\theta}_w\left(\theta\bar{\theta}_w+1\right)^2\theta'^2+\left(\theta\bar{\theta}_w+1\right)^3\theta''\right)$$

$$\frac{\partial q_r}{\partial y} = -\frac{16\sigma^* T^4}{3\alpha^*}\frac{m+1}{2}\frac{u_0 x^{m-1}}{\upsilon}\bar{\theta}_w$$
$$\left(3\bar{\theta}_w\left(\theta\bar{\theta}_w+1\right)^2\theta'^2+\left(\theta\bar{\theta}_w+1\right)^3\theta''\right) \qquad (8)$$

It is also obtained that:

$$\frac{1}{\mu} = d_2(T-T_r) = \frac{1}{\mu_\infty}((T-T_\infty)\gamma+1) = \frac{1}{\mu_\infty}((T_w-T_\infty)\gamma\theta+1) =$$

$$\frac{(T_w-T_\infty)\gamma}{\mu_\infty}\left(\theta+\frac{1}{(T_w-T_\infty)\gamma}\right) = b(T_w-T_\infty)(\theta+\theta_c)$$

$$\frac{1}{\mu} = b(T_w-T_\infty)(\theta+\theta_c) \qquad (9)$$

$$\frac{1}{k_*} = \frac{1}{k_\infty}(1+k(T-T_\infty)) = \frac{1}{k_\infty}(1+k(T_w-T_\infty)\theta) =$$

$$\frac{k}{k_\infty}(T_w-T\infty)\left(\theta+\frac{1}{k(T_w-T_\infty)}\right) = \alpha(\theta+\theta_r)$$

Table 1: Comparison of f'(η) from Devi and Gururaj[8] result with the current research for and M = 0.4 and M = 0.8

f'(η)/η	M = 2.0			M = 4.0		
	Devi and David	Current work	Difference	Devi and David	Current work	Difference
0.0	1.00000000	1.00000000	0.0000000	1.00000000	1.00000000	0.00000000
0.4	0.32339773	0.32339773	0.0000000	0.23321715	0.23381716	0.00000001
0.8	0.10736922	0.10736922	0.0000000	0.05612983	0.05652983	0.00000000
1.2	0.03668281	0.03668272	0.0000009	0.01399448	0.01379478	0.00000030
1.6	0.01282269	0.01282269	0.0000000	0.00367791	0.00307801	0.00000010
2.0	0.00466227	0.00466228	0.0000010	0.00096220	0.00066210	0.00000010
2.4	0.00175143	0.00175154	0.0000011	0.00029220	0.00069250	0.00000030
2.8	0.00060943	0.00060963	0.0000020	0.00008152	0.00078202	0.00000050
3.2	0.00023224	0.00023224	0.0000000	0.00003794	0.00023814	0.00000020
3.6	0.00011875	0.00011875	0.0000000	0.00007730	0.00007731	0.00000001

$$\frac{1}{k_*} = \alpha\left(\theta + \theta_r\right) \quad (10)$$

Viscosity factor $b = \dfrac{\gamma}{\mu_\infty} \begin{cases} >0 \text{ for liquids} \\ <0 \text{ for gases} \end{cases}$

$$\theta_c = \frac{1}{\left(T_w - T_\infty\right)\gamma}, \ \theta_r = \frac{1}{k\left(T_w - T_\infty\right)}, \ \alpha = \frac{k}{k_\infty}\left(T_w - T_\infty\right)$$

Then:

$$v = -\frac{\partial\psi}{\partial x} = -\sqrt{\frac{m+1}{2}}\sqrt{u_0 x^{m-1}}\left(f + \frac{m-1}{m+1}\eta f'\right)$$

And:

$$u = \frac{\partial\psi}{\partial y} = u_0 x^m f'$$

Thus, continuity Eq. 1 implies, therefore, the non-dimensional variables appropriate for the problem under consideration are:

$$\eta = y\sqrt{\frac{u_0}{\upsilon}}, v = -\sqrt{u_0\upsilon}f, u = u_0 x f' \quad (11)$$

Equation 2-4 and boundary condition (Eq. 6) becomes:

$$\frac{\theta_c}{\theta+\theta_c}f'' + ff'' - f'^2 - \frac{\theta_c}{\left(\theta+\theta_c\right)^2}\theta'f' + Grt\,\theta + Grc\phi - Mf' = 0 \quad (12)$$

$$\frac{\theta_r}{\theta+\theta_r}\theta'' + Prf\theta' - \frac{\theta_c}{\left(\theta+\theta_c\right)^2}\theta'^2 + \frac{4\bar\theta_w}{3R}\left(\begin{array}{c}3\bar\theta_w\theta'^2 + \\ \left(\bar\theta_w\theta+1\right)\theta''\end{array}\right)\left(\bar\theta_w\theta+1\right)^2 = 0 \quad (13)$$

$$\phi'' + Scf\phi' + \beta Sc\phi = 0 \quad (14)$$

$$f(0) = 0, f'(0) = 1, \phi(0) = 1, \theta(0) = 1 : y = 0$$
$$\theta(\eta) \to 0, \varnothing(\eta) \to 0, f'(\eta) \to 0 : \eta \to \infty \quad (15)$$

Where:

$\theta_c = 1/\left(T_w - T_\infty\right)\gamma$: The viscosity measuring parameter

$\theta_r = 1/k\left(T_w - T_\infty\right)$: The thermal conductivity term

$R = k\alpha^*/4\sigma^*T4$: The heat transfer rate

$M = \sigma B_0^2/\rho u_0$: The magnetic term

$\mu c_p/k$: The Prandtl number

$Grt = g\beta_r\left(T_w - T_\infty\right)/$: The thermal buoyancy

$\rho x u_0^2$

$Grc = g\beta_r\left(C_w - C_\infty\right)/$: The mass buoyancy

$\rho x u_0^2$

$Sc = \mu/Dm$: The Schmidt number

$\beta = A/\upsilon u_0$: The reaction parameter

Numerical solution of the problem: Computational solution to the dimension less (Eq. 12-14) along with the boundary conditions (Eq. 15) are gotten by coupled trapezoid method with Runge-Kutta seventh-eighth of continuous order schemeand Richardson extrapolation improvement[27-29]. A shooting method is used first to change the derivatives to differential equations of first order. The non-magnetic solution is taken as the primary guess; the Euler iterative techniquesis used continuously until it convergence within the given precision. The following are prescribed parametersin the study β, Grt, Grc, M, R, θ_w, φ, θ_c, θ_r Sc and Pr. The initial guesses with the equation was solved by Thoma's algorithm. The computation was carried out using MAPLE 18.

Special cases: In nonexistence of radiation term, the numerical value is compared to that by Devi and Gururaj[8] as illustrated through Table 1 and 2. From the tables, it is noticed that the results are in good agreement with that by Devi and Gururaj[8]. When magnetic

Table 2: Comparison of θ(η) from Devi and David result with the current research for M = 0.4 and M = 0.8

θ (η)/η	M = 2.0			M = 4.0		
	Devi and David	Current work	Difference	Devi and David	Current work	Difference
0.0	1.000000	1.000000	0.000000	1.000000	1.000000	0.000000
0.4	0.326922	0.326921	0.000001	0.277864	0.277864	0.000000
0.8	0.106878	0.106877	0.000001	0.077208	0.077208	0.000000
1.2	0.034941	0.034938	0.000003	0.021453	0.021453	0.000000
1.6	0.011423	0.011420	0.000003	0.005961	0.005961	0.000000
2.0	0.003734	0.003730	0.000004	0.001656	0.001656	0.000000
2.4	0.001221	0.001215	0.000006	0.000460	0.000460	0.000000
2.8	0.000399	0.000392	0.000007	0.000128	0.000127	0.000000
3.2	0.000130	0.000122	0.000008	0.000036	0.000035	0.000001
3.6	0.000043	0.000032	0.000011	0.000010	0.000008	0.000002

field is absent, the results obtained in the study takes the form Okedoye *et al.*[30]. In the absence of variable conductivity and magnetic field, the study is similar to that by Okedoye[11] in the absence of radiation effect with constant thermal conductivity.

Validity of results: We compare this results with the result by Devi and Gururaj[8] with our numerical result for M = 2 and M = 4. It is observed from Table 1 and 2 that the numerical values of velocity f'(η) and θ(η) are in good agreement as shown in tables.

There is good agreement in the comparison as presented in the tables. In contrast to the above numerical solution presented here, the Prandtl number used is one corresponding to the one for plasma (Pr = 0.71) and Schmidt number corresponding to that of water vapour (Sc = 0.62).

RESULTS AND DISCUSSION

The solutions to the dimensionless formulated equations governing the flow are computationally obtained for different physical parameters values entrenched in the model. The computational results are illustrated graphically for the various flow fields as showed in Fig. 2-15.

The impact of viscosity measuring termon the dimensionless momentum f'(η) and concentration field φ(η) are seen through Table 3. As viscosity measuring parameter increases in magnitude, velocity decreases. Furthermore, it is interesting to notice that the rise in viscosity measuring term decrease the momentum boundary layer thickness. While rises in magnitude of viscosity measuring parameter θ_c increases the concentration distribution. Thus, confirming the fact that the viscosity measuring parameter enhances the concentration boundary layer thickness. Table 4 shows the influence of viscosity measuring term θ_c over the temperature θ(η) and the effect of thermal conductivity measuring parameter θ_r on the dimensionless velocity field f'(η), respectively. Viscosity measuring parameter θ_r increases in magnitude, temperature increases. Also, as previously noted for concentration distribution increase in
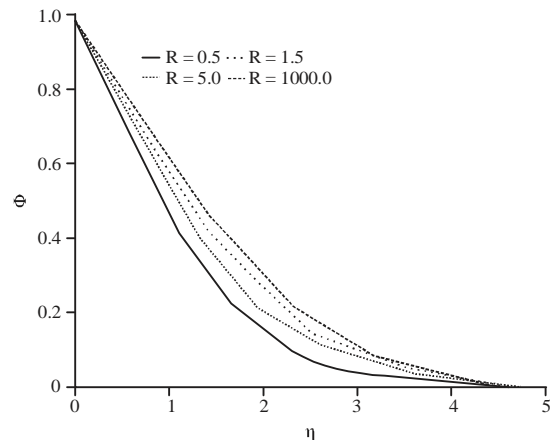

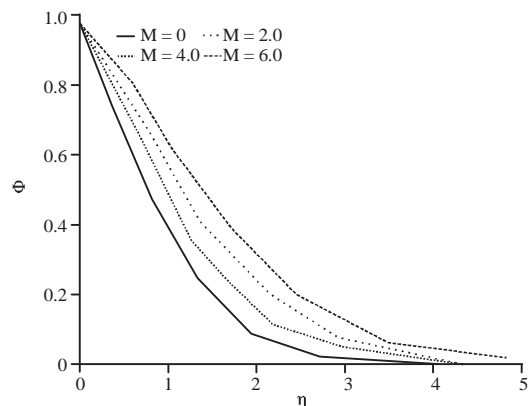Fig. 2: Concentration distributions

Fig. 3: Concentration distributions profile for various radiation parameters profile for various

viscosity measuring parameter enhances the temperature boundary layer thickness. While increases in magnitude of thermal conductivity measuring parameter increases the velocity distribution. Also, it is noticed that the thermal conductivity measuring term enhances the flow rate boundary layer thickness. The influence of thermal conductivity measuring term on both concentration and heat distributions, respectively is shown in Table 5. From this table increase in thermal conductivity brings about

Table 3: Effect of viscosity measuring term on f'(η) and φ(η)

	f'(η)				φ(η)			
η	$\theta_c = 0.1$	$\theta_c = 5$	$\theta_c = 100$	$\theta_c = 200$	$\theta_c = 0.1$	$\theta_c = 5$	$\theta_c = 100$	$\theta_c = 200$
0	1.00000	1.00000	1.00000	1.00000	1.00000	1.00000	1.00000	1.00000
0.4	1.53506	1.29686	1.27334	1.27210	0.77717	0.79494	0.79656	0.79665
0.8	1.25357	1.22898	1.21920	1.21864	0.55589	0.58360	0.58626	0.58641
1.2	0.97260	1.03063	1.03390	1.03410	0.36964	0.39755	0.40035	0.40051
1.6	0.72876	0.80879	0.81759	0.81807	0.23147	0.25384	0.25615	0.25628
2.0	0.52800	0.60586	0.61502	0.61553	0.13821	0.15370	0.15532	0.15540

Table 4: Impact of viscosity measuring and thermal conductivity parameters on θ(η) and φ(η), respectively

	θ(η)				f'(η)			
η	$\theta_c = 0.1$	$\theta_c = 5$	$\theta_c = 100$	$\theta_c = 200$	$\theta_c = 0.1$	$\theta_c = 5$	$\theta_c = 100$	$\theta_c = 200$
0	1.00000	1.00000	1.00000	1.00000	1.00000	1.00000	1.00000	1.00000
0.4	0.88652	0.89010	0.89044	0.89046	1.40490	1.40355	1.41708	1.41714
0.8	0.76552	0.77251	0.77318	0.77322	1.24810	1.24653	1.27642	1.27654
1.2	0.64136	0.65082	0.65175	0.65180	0.98577	0.98567	1.03351	1.03368
1.6	0.51951	0.53011	0.53116	0.53122	0.73476	0.73755	0.80053	0.80072
2	0.40577	0.41613	0.41717	0.41723	0.52260	0.52906	0.60006	0.60025

Table 5: Effect of thermal conductivity parameters on θ(η) and θ(η), respectively

|	φ(η)				θ(η)			
η	$\theta_r = 1$	$\theta_r = 20$	$\theta_r = 30$	$\theta_r = 40$	$\theta_r = 1$	$\theta_r = 20$	$\theta_r = 30$	$\theta_r = 40$
0	1.00000	1.00000	1.00000	1.00000	1.00000	1.00000	1.00000	1.00000
0.4	0.79016	0.79007	0.78470	0.78468	0.88781	0.88641	0.89440	0.89445
0.8	0.57653	0.57634	0.56659	0.56655	0.76572	0.76328	0.78220	0.78229
1.2	0.39153	0.39124	0.37894	0.37890	0.63726	0.63443	0.66655	0.66669
1.6	0.25060	0.25020	0.23744	0.23740	0.50783	0.50568	0.55154	0.55171
2	0.15308	0.15261	0.14108	0.14104	0.38438	0.38425	0.44160	0.44178
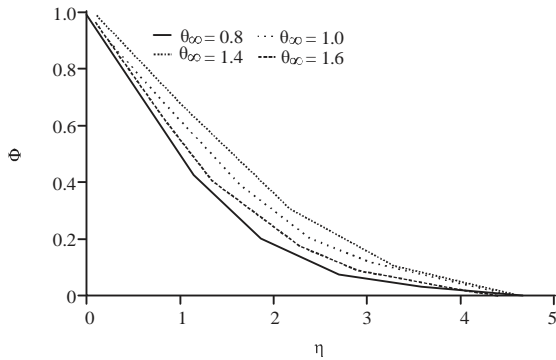
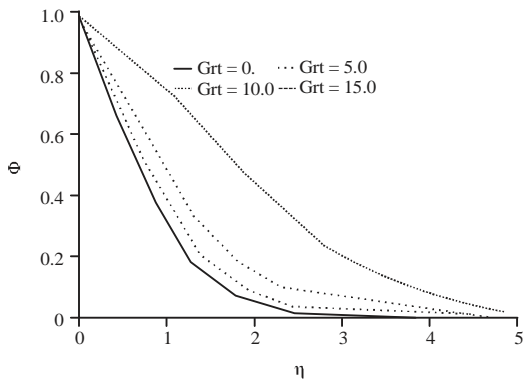Fig. 4: Concentration distributions profile for various θ_w

Fig. 5: Concentration distributions profile for various Grt
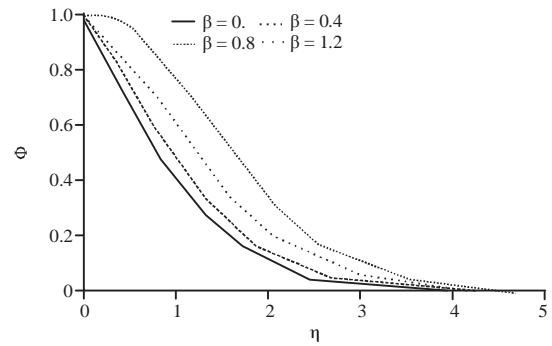

Fig. 6: Concentration distributions profile for various β
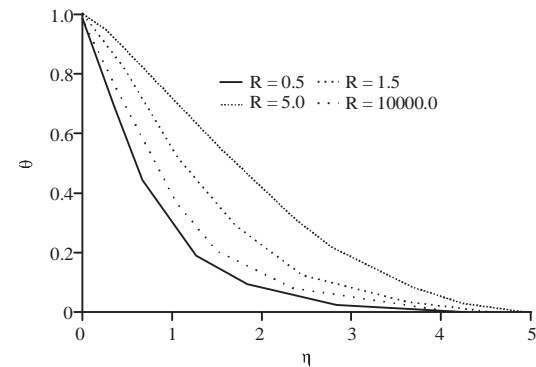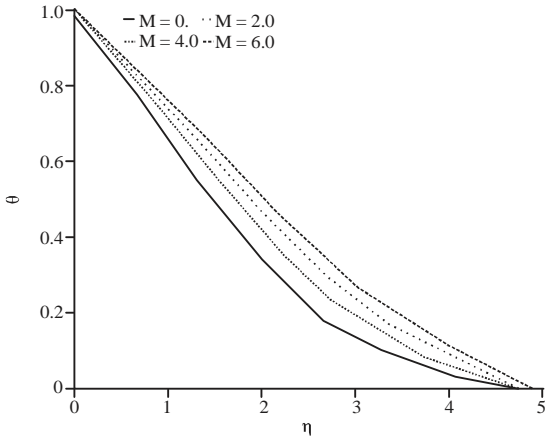

Fig. 7: Temperature distributions profile for various R

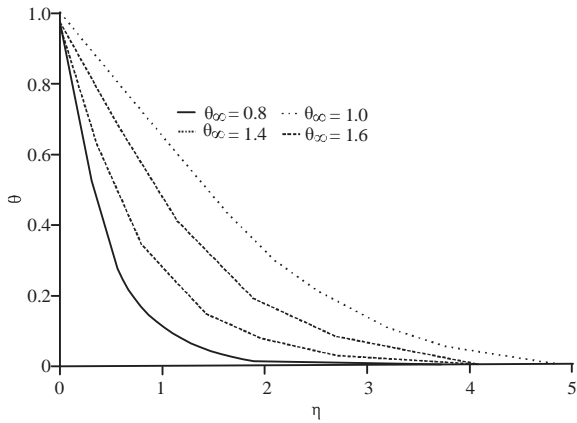Fig. 8: Temperature distributions profile for various Grt
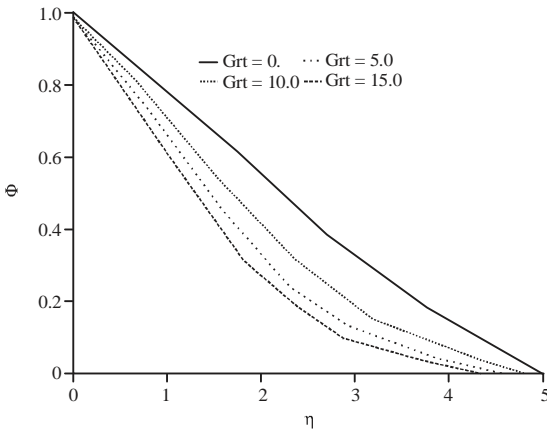

Fig. 9: Temperature distributions profile for various θ_w

Fig. 10: Temperature distributions profile for various Grt

Fig. 11: Velocity distributions profile for various β

Fig. 12: Velocity distributions profile for various R
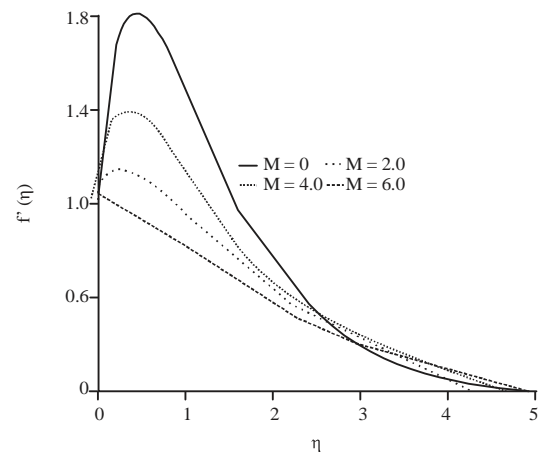
Fig. 13: Velocity distributions for various M

decrease in concentration distribution. This is so because increase in temperature will enhance consumption of more chemical species to support the rise in the momentum f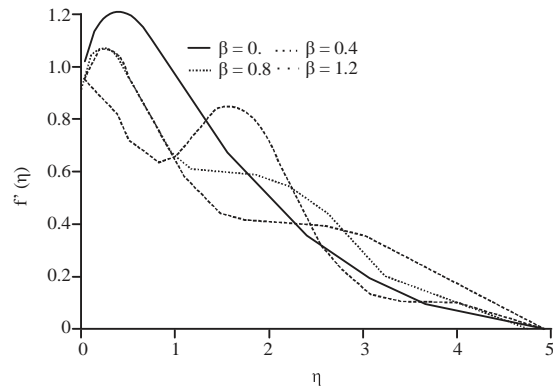low profile. Whereas increase in thermal conductivity result to increase in temperature distribution. Thus, it is worth to mention that increase in thermal conductivity enhances the temperature and heat boundary layer.
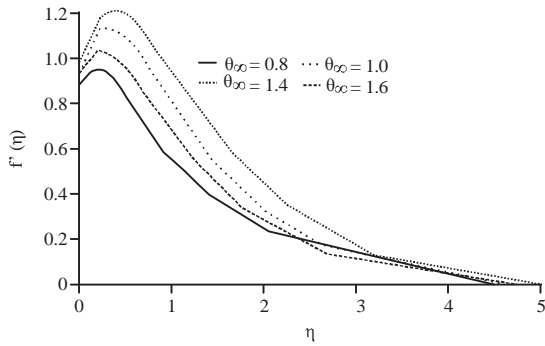
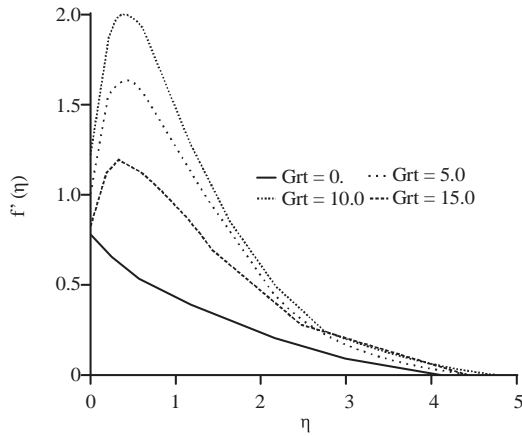Fig. 14: Velocity distributions profile for various θ_w

Fig. 15: Velocity distributions profile for various Grt

We displayed the impact of magnetic interaction term (M) and radiation term (R) on the concentration distributions in Fig. 2 and 3. Concentration distribution is encouraged with either rise in the radiation or magnetic field term. This implies that the species boundary layer thickens with a rise in R and M. Increase in surface temperature and thermal buoyancy enhances the concentration field. The mass distribution is enhanced with variational rise in the surface temperature and thermal Grashof number as shown in Fig. 4 and 5, respectively. While Fig. 6 shows that mass distribution speedup with a rise in the generative chemical reaction ($\beta > 0$). The consequence of thermal radiation term® over the dimensionless heat $\theta(\eta)$ is seen through Fig. 7. It is observed that the influence of radiation term is to decrease the heat distribution is the system. It elucidates that the thickness in the boundary layer of the energy equation R is reducing as values is enhances. The response of heat source term in the heat equation to a rise in the magnetic field M over the flow heat $\theta(\eta)$ is depicted with the aid of Fig. 8. Enhancing the magnetic field term M encourages Lorentz force in the flow which then resulted into rise in the heat profile. This described the fact that increase in the Lorentz force

boosted the temperature source term in the energy balance equation. The effect of stretching surface temperature term θ_w on the dimensionless heat $\theta(\eta)$ is presented as Fig. 9 Rising in the surface heat term θ_w is seen to have increasing effect on the temperature distribution. Figure 10 illustrates thermal buoyancy effect on the temperature field. Boosting the thermal Grashof number (Grt) decreases the temperature distribution, this describing the impact of Grt on the bulk temperature. Decreasing in the bulk temperature influence the heat source parameter in the system to increases thereby enhances the heat profile. Figure 12 and 13 portray the graphical result of the momentum $f'(\eta)$ for various values of radiation term R and magnetic interaction parameter M. It is observed that as the parameter values and rises, the fluid velocity distribution reduces to $f'(\eta)$ show influence of radiation and magnetic field terms on the fluid flow rate in under different variable properties. The profiles decelerated as the parameters values in boosting. The action of surface temperature and thermal buoyancy on non-dimensional velocity distribution in plotted in Fig. 14 and 15, respectively. It is obtained from the plots that an increase in either θ_w or Grt increases the flow momentum and enhances thickness of the flow boundary layer as seen due to a rise in the values of θ_w or Grt.

Skin friction, heat and mass gradient: We now move to examining some important fluid parameters that are of importance to this work. Such parameters include skin friction, Sherwood and Nusselt numbers coefficient. We therefore, denote and define, respectively, Skinfriction, Nusselt and Sherwood numbers as:

$$c_f = \frac{T_f}{\rho u_\omega v_\omega}, \qquad T_f = \mu \frac{du}{dy}\bigg|_{y=0} \qquad \Rightarrow c_f = -\frac{d^2}{d\eta^2} f(0)$$

The heat transfer at the wall is computed from Fourier's law:

$$Nu = \frac{q_\omega v}{(T_\omega - T_\infty) K v_\omega}, \qquad q_\omega = -D \frac{dC}{dy}\bigg|_{y=0} \qquad \Rightarrow Sh = -\frac{d}{d\eta} \phi(0)$$

And mass transfer rate at wall:

$$Sh = \frac{J_\omega v}{(J_\omega - J_\infty) D v_\omega}, \qquad J_\omega = -D \frac{dC}{dy}\bigg|_{y=0}, \qquad \Rightarrow Sh = -\frac{d}{d\eta} \phi(0)$$

Table 6 presents the effect of the parameters Grt, Grc, M, θ_c, θ_r, θ_w, R, β on the wall shear stress c_f, Sherwood number Sh and wall heat gradient Nu for Sc = 0.62, Pr = 0.71 and $\epsilon = 0.01$. From the table, the heat and species buoyancy, surface temperature and reaction parameter rises the coefficient of skin friction. But

Table 6: Skin friction, gradient of energy and species transfer

Grt	Grc	M	θ_c	θ_r	θ_w	R	β	c_f	Sh	Nu
0.0	2.0	2.0	0.6	0.8	1.5	5.0	0.4	-1.08182	0.15662	0.20182
5.0	2.0	2.0	0.6	0.8	1.5	5.0	0.4	2.57279	0.49550	0.26680
10.0	2.0	2.0	0.6	0.8	1.5	5.0	0.4	5.86878	0.64549	0.31049
15.0	2.0	2.0	0.6	0.8	1.5	5.0	0.4	8.92490	0.74383	0.34283
5.0	0.0	2.0	0.6	0.8	1.5	5.0	0.4	1.25845	0.43265	0.25230
5.0	2.0	2.0	0.6	0.8	1.5	5.0	0.4	2.57279	0.49550	0.26680
5.0	6.0	2.0	0.6	0.8	1.5	5.0	0.4	4.99743	0.58459	0.28893
5.0	12.0	2.0	0.6	0.8	1.5	5.0	0.4	8.32460	0.67732	0.31370
5.0	2.0	0.0	0.6	0.8	1.5	5.0	0.4	4.83244	0.62428	0.30337
5.0	2.0	2.0	0.6	0.8	1.5	5.0	0.4	2.57279	0.49550	0.26680
5.0	2.0	4.0	0.6	0.8	1.5	5.0	0.4	0.95431	0.38386	0.24054
5.0	2.0	6.0	0.6	0.8	1.5	5.0	0.4	-0.27328	0.28910	0.22220
5.0	2.0	2.0	0.1	0.8	1.5	5.0	0.4	5.95466	0.52346	0.27171
5.0	2.0	2.0	50.0	0.8	1.5	5.0	0.4	1.34764	0.47182	0.26257
5.0	2.0	2.0	100.0	0.8	1.5	5.0	0.4	1.33821	0.47158	0.26252
5.0	2.0	2.0	2000.0	0.8	1.5	5.0	0.4	1.32921	0.47135	0.26248
5.0	2.0	2.0	0.6	0.0	1.5	5.0	0.4	2.56594	0.48865	0.26652
5.0	2.0	2.0	0.6	0.1	1.5	5.0	0.4	2.56234	0.48889	0.27025
5.0	2.0	2.0	0.6	15.0	1.5	5.0	0.4	2.59287	0.50270	0.25392
5.0	2.0	2.0	0.6	40.0	1.5	5.0	0.4	2.59302	0.50275	0.25381
5.0	2.0	2.0	0.6	0.8	0.8	5.0	0.4	1.24735	0.25659	1.79983
5.0	2.0	2.0	0.6	0.8	1.0	5.0	0.4	1.78345	0.33036	1.12815
5.0	2.0	2.0	0.6	0.8	1.2	5.0	0.4	2.22678	0.40798	0.56860
5.0	2.0	2.0	0.6	0.8	1.4	5.0	0.4	2.48936	0.47156	0.33215
5.0	2.0	2.0	0.6	0.8	1.5	0.5	0.4	2.57279	0.49550	0.26680
5.0	2.0	2.0	0.6	0.8	1.5	1.5	0.4	2.33973	0.42677	0.44214
5.0	2.0	2.0	0.6	0.8	1.5	5.0	0.4	2.06203	0.36876	0.70642
5.0	2.0	2.0	0.6	0.8	1.5	2000.0	0.4	1.78543	0.33059	1.12413
5.0	2.0	2.0	0.6	0.8	1.5	5.0	0.0	2.51671	0.68072	0.26486
5.0	2.0	2.0	0.6	0.8	1.5	5.0	0.4	2.57279	0.49550	0.26680
5.0	2.0	2.0	0.6	0.8	1.5	5.0	0.8	2.65253	0.25056	0.26982
5.0	2.0	2.0	0.6	0.8	1.5	5.0	1.2	2.78307	0.12245	0.27518

thermal and viscosity conductivity measuring heat transport and parameters reduces the coefficient skin friction c_f. It is also noticed that the dimensionless wall heat transport gradient enhances with rises in the thermal and mass buoyancy, thermal conductivity measuring parameter and heat transfer rate but decrease with viscosity measuring parameter, surface temperature, magnetic and chemical reaction parameters. While surface temperature, thermal and mass buoyance are found to enhance the mass transfer rate at the wall and decreases with Hartmann number, thermal and viscosity conductivity measuring parameter, heat transfer rate and chemical reactivity terms.

CONCLUSION

The following conclusions are made in view of the above obtained results. It is noticed that the magnetic field decelerate the momentum and enhances temperature distribution in the system under consideration. It is seen that the term that increases the heat source term diminishes the fluid viscosity. Temperature is found to reduce due to the radiation term effect while it is found to increase with the increasing surface heat parameter. The thickness of heat boundary layer reduces significantly as Prandtl number rises. The skin friction and the fluid flow rate decreased by the velocity exponent term. On the other hand, heat diffusion is enhanced by the velocity exponent

parameter. It is obtained that for encouraging radiation parameter R, the dimensionless rate of heat transfer decreases.

NOMENCLATURE

(x) : Variable applied magnetic induction
θ : Dimensionless temperature
T : Temperature of t
m : Velocity exponent parameter
C_p : Heat capacity
P : Pressure of the fluid
k_* : Thermal conductivity
ρ : Density of the fluid
ψ : Stream function
υ : Kinematic viscosity
T_w : Heated plate temperature
B_0 : Constant applied magnetic induction
$T\infty$: Fluid ambient temperature.
U, v : Velocity component of fluid in x and y direction

REFERENCES

01. Seth, G.S., S.M. Hussain and J.K. Singh, 2011. MHD couette flow of class-II in a rotating system. J. Applied Math. Bioinf., 1: 31-54.

02. Salawu, S.O. and S.I. Oke, 2018. Inherent irreversibility of exothermic chemical reactive third-grade poiseuille flow of a variable viscosity with convective cooling. J. Applied Comput. Mech., 4: 167-174.

03. Salawu, S.O. and A.M. Okedoye, 2018. Thermodynamic second law analysis of hydromagnetic gravity-driven two-step exothermic chemical reactive flow with heat absorption along a channel. Iran. J. Energy Environ., 9: 114-120.

04. Hassan, A.R., J.A. Gbadeyan and S.O. Salawu, 2017. The effects of thermal radiation on a reactive hydromagnetic internal heat generating fluid flow through parallel porous plates. Proceedings of the International Conference on Applied Mathematics, Modeling and Computational Science, August 20-25, 2017, Springer, Cham, Switzerland, pp: 183-193.

05. Fetecau, C., C. Fetecau, M. Kamran and D. Vieru, 2009. Exact solutions for the flow of a generalized Oldroyd-B fluid induced by a constantly accelerating plate between two side walls perpendicular to the plate. Int. J. Non-Newtonian Fluid Mech., 156: 189-201.

06. Hayat, T., S.A. Shehzad and A. Alsaedi, 2013. Three-dimensional stretched flow of Jeffrey fluid with variable thermal conductivity and thermal radiation. Applied Math. Mech., 34: 823-832.

07. Salawu, S.O., H.A. Ogunseye and A.M. Olanrewaju, 2018. Dynamical analysis of unsteady poiseuille flow of two-step exothermic non-Newtonian chemical reactive fluid with variable viscosity. Int. J. Mech. Eng. Technol., 9: 596-605.

08. Devi, S.A. and A.D.M. Gururaj, 2012. Effects of variable viscosity and nonlinear radiation on MHD flow with heat transfer over a surface stretching with a power-law velocity. Adv. Applied Sci. Res., 3: 319-334.

09. Gitima, P., 2012. Effect of variable viscosity and thermal conductivity of micropolar fluid in a porous channel in presence of magnetic field. Int. J. Basic Sci. Social, 1: 69-77.

10. Hazarika, G.C. and U.S.G. Ch, 2012. Effects of variable viscosity and thermal conductivity on MHD flow past a vertical plate. Matematicas: Ensenanza Universitaria, 20: 45-54.

11. Okedoye, A.M., 2015. On the unsteady free convective flow with Radiative heat transfer of Sisko fluid. IJISET. Int. J. Innovative Sci. Eng. Technol., 2: 427-437.

12. Salawu, S.O., 2018. Analysis of third-grade heat absorption hydromagnetic exothermic chemical reactive flow in a Darcy-forchheimer porous medium with convective cooling. WSEAS Transac. Math., 17: 280-289.

13. Abdou, M.M.M., 2010. Effect of radiation with temperature dependent viscosity and thermal conductivity on unsteady a stretching sheet through porous media. Nonlinear Anal. Modell. Control, 15: 257-270.

14. Salem, A.M., 2007. Variable viscosity and thermal conductivity effects on MHD flow and heat transfer in viscoelastic fluid over a stretching sheet. Phys. Let. A., 369: 315-322.

15. Chen, C.H., 2006. Effect of viscous dissipation on heat transfer in a non-Newtonian liquid film over an unsteady stretching sheet. J. Non-Newtonian Fluid Mech., 135: 128-135.

16. Elbashbeshy, E.M., 1998. Heat transfer over a stretching surface with variable surface heat flux. J. Phys. D. Applied Phys., 31: 1951-1954.

17. Elbashbeshy, E.M.A. and M.A.A. Bazid, 2004. Heat transfer over an unsteady stretching surface. Heat Mass Transfer, 41: 1-4.

18. Afify, A.A., 2009. Similarity solution in MHD: Effects of thermal diffusion and diffusion thermo on free convective heat and mass transfer over a stretching surface considering suction or injection. Commun. Nonlinear Sci. Numer. Simul., 14: 2202-2214.

19. Abdou, M.M.M. and S.M.M. El-Kabeir, 2007. Magnetohydrodynamics and radiative effects on free convection flow of fluid with variable viscosity from a vertical plate through a porous medium. J. Porous Media, 10: 503-556.

20. Yurusoy, M., 2006. Unsteady boundary layer flow of power-law fluid on stretching sheet surface. Int. J. Eng. Sci., 44: 325-332.

21. Grubka, L.J. and K.M. Bobba, 1985. Heat transfer characteristics of a continuous, stretching surface with variable temperature. J. Heat Transfer, 107: 248-250.

22. Ali, M.E., 2006. The effect of variable viscosity on mixed convection heat transfer along a vertical moving surface. Int. J. Thermal Sci., 45: 60-69.

23. Kafoussias, N.G., 1992. MHD thermal-diffusion effects on free-convective and mass-transfer flow over an infinite vertical moving plate. Astrophys. Space Sci., 192: 11-19.

24. Salawu, S.O. and E.O. Fatunmbi, 2017. Inherent irreversibility of hydromagnetic third-grade reactive poiseuille flow of a variable viscosity in porous media with convective cooling. J. Serbian Soc. Comput. Mech., 11: 46-58.

25. Salawu, S.O. and M.S. Dada, 2018. Lie group analysis of soret and dufour effects on radiative inclined magnetic pressure-driven flow past a Darcy-forchheimer medium. J. Serbian Soc. Comput. Mech., 12: 108-125.

26. Salawu, S.O. and E.O. Fatunmbi, 2017. Inherent irreversibility of hydromagnetic third-grade reactive poiseuille flow of a variable viscosity in porous media with convective cooling. J. Serbian Soc. Comput. Mech., 11: 46-58.

27. Sharidan, S., M. Mahmood and I. Pop, 2006. Similarity solutions for the unsteady boundary layer flow and heat transfer due to a stretching sheet. Applied Mech. Eng., 11: 647-654.

28. Kareem, R.A., S.O. Salawu and J.A. Gbadeyan, 2018. Numerical analysis of Non-uniform heat source/sink in a radiative micropolar variable electric conductivity fluid with dissipation joule heating. Am. J. Appl. Math., 6: 34-41.

29. Ascher, U.M. and L.R. Petzold, 1998. Computer Methods for Ordinary Differential Equations and Differential-Algebraic Equations. SIAM, Philadelphia, USA., ISBN-13: 9780898714128, Pages: 314.

30. Okedoye, A.M., V.A. Akinrinmade and Y.S. Onifade, 2017. Heat and mass transfer MHD flow of a Sisko fluid in porous medium. Confluence J. Pure Appl. Sci., 11: 324-333.